cells

MDPI

Article

circRTN4 Suppresses Bovine Adipogenesis via the miR-205/Lin9 Axis

Yue Liu [1,†], Taotao Yan [1,†], Xuanjin Wang [1], Li Sun [1], Zhuoyuan He [1], Sihuan Zhang [2], Chuanying Pan [1], Yang Li [1], Xianyong Lan [1,*] and Enhui Jiang [1,*]

[1] Key Laboratory of Animal Genetics, Breeding and Reproduction of Shaanxi Province, College of Animal Science and Technology, Northwest A&F University, Yangling 712100, China; liuyue527@nwsuaf.edu.cn (Y.L.)
[2] College of Animal Science and Technology, Anhui Agricultural University, Hefei 230036, China
* Correspondence: lanxianyong79@nwsuaf.edu.cn (X.L.); jiangenhui666@nwafu.edu.cn (E.J.)
† These authors contributed equally to this work.

Highlights

What are the main findings?

- Identified circRTN4 from RTN4 exons 4 and 5; expressed in bovine adipose tissue and upregulated during differentiation.
- circRTN4 affects preadipocyte proliferation, apoptosis, and differentiation via the miR-205/Lin9 regulatory axis.

What is the implication of the main finding?

- The circRTN4/miR-205/Lin9 axis provides insights into bovine preadipocyte regulation.
- circRTN4 is a potential target for modulating bovine adipose tissue development.

Abstract

Adipocyte proliferation and differentiation are important processes underlying bovine adipose tissue development. We identified a novel circular RNA derived from exons 4 and 5 of the RTN4 gene, designated as circRTN4, which was upregulated during bovine adipocyte differentiation, and investigated its effects on preadipocyte proliferation, apoptosis, and differentiation. The circRTN4/miR-205/Lin9 regulatory axis was explored by dual-luciferase reporter assays, RNA interference, and overexpression. circRTN4, derived from exons 4 and 5 of the RTN4 gene, was expressed in adipose tissue and resistant to RNase R digestion. Although the translation potential of circRTN4 was evaluated, no FLAG-tagged peptide was detected in the expression assay. Overexpression of circRTN4 significantly inhibited preadipocyte proliferation and differentiation while promoting apoptosis. Further analyses supported a potential regulatory relationship between circRTN4, miR-205, and Lin9. Lin9 suppressed proliferation and differentiation and enhanced apoptosis. Overall, these findings suggest that circRTN4 may regulate bovine preadipocyte functions through the miR-205/Lin9 regulatory axis.

Keywords: circRTN4; ceRNA; adipocytes; translation assay

Check for updates

Academic Editor: Victoriano Baladrón

Received: 3 September 2026
Revised: 8 October 2026
Accepted: 10 November 2026
Published: 18 November 2026

Copyright: © 2026 by the authors. Licensee MDPI, Basel, Switzerland. This article is an open access article distributed under the terms and conditions of the Creative Commons Attribution (CC BY) license.

1. Introduction

Adipose tissue development is an important component of bovine growth and metabolism and is closely associated with economically relevant production traits. Adipocyte proliferation, differentiation, and lipid accumulation are fundamental processes underlying adipose tissue development. Therefore, elucidating the molecular mechanisms regulating

bovine preadipocyte proliferation and adipogenic differentiation is important for understanding bovine adipose biology and fat deposition [1,2]. In beef cattle production, the amount and distribution of adipose tissue are important determinants of carcass composition and meat quality. Although appropriate intramuscular fat deposition is associated with desirable sensory characteristics, excessive subcutaneous and visceral fat accumulation can negatively affect production efficiency and carcass value [3]. Therefore, elucidating the molecular regulatory mechanisms underlying the proliferation, differentiation, and apoptosis of bovine preadipocytes holds significant scientific value for understanding the regulation of bovine adipose tissue development and fat deposition.

Adipogenesis is a highly ordered biological process involving the proliferation of preadipocytes, mitotic clonal expansion, terminal differentiation, and lipid droplet accumulation, which is precisely regulated by multiple transcription factors, signaling pathways, and non-coding RNAs (ncRNA) [4–6]. Recently, circular RNAs (circRNAs), as a class of covalently closed, highly stable non-coding RNA molecules, have been demonstrated to be extensively involved in the regulatory network of mammalian adipogenesis [7,8]. circRNAs primarily function at the post-transcriptional level to influence target gene expression by acting as miRNA sponges, interacting with RNA-binding proteins, or directly encoding small peptides [9]. A large number of circRNAs have been identified and demonstrated to regulate the proliferation and differentiation of preadipocytes. For example, circMEF2C (2, 3) reflected that it participates in promoting proliferation and inhibiting adipogenic differentiation in porcine intramuscular preadipocytes and murine C3H10T1/2 cells [10]. CircDOCK7 facilitates the proliferation and adipogenic differentiation of chicken abdominal preadipocytes through the gga-miR-301b-3p/ACSL1 axis [11]. Furthermore, circBDP1 acts as a ceRNA for miR-181b and miR-204 to regulate their common target SIRT1 and the miR-204-specific target TRARG1, thereby promoting bovine preadipocyte proliferation and differentiation [12]. These studies indicate that circRNAs can participate in the regulation of adipocyte proliferation and differentiation in livestock, highlighting their potential roles in bovine adipose biology.

Although the functions of circRNAs in adipose development have gained increasing attention, the regulatory roles of many bovine adipocyte-associated circRNAs remain poorly understood. In our preliminary analysis of circRNA expression during bovine preadipocyte adipogenic differentiation, circRTN4 emerged as a candidate circRNA for further functional investigation. RTN4 encodes an endoplasmic reticulum transmembrane protein that is primarily involved in the inhibition of neuronal axon growth and the regulation of apoptosis [13]. In addition, circRTN4 has been reported to promote tumor growth and liver metastasis in pancreatic ductal adenocarcinoma through the circRTN4/miR-497-5p/HOTTIP regulatory pathway [14]. However, the biological function and molecular mechanism of circRTN4 in bovine adipocytes have not yet been characterized. To explore the potential molecular mechanism underlying circRTN4 function, candidate miRNAs potentially interacting with circRTN4 were first identified by bioinformatic prediction and subsequently screened by RT-qPCR, leading to the selection of miR-205. Candidate downstream targets of miR-205 were then predicted and further screened by RT-qPCR, leading to the selection of Lin9 as a potential downstream target. Lin9 is a core component of the DREAM complex, which represses the transcription of cell-cycle-related genes and promotes cell-cycle exit [15], making it a biologically relevant candidate for investigating the potential regulation of bovine preadipocyte proliferation. In the present study, we investigated the expression, biological function, and potential molecular mechanism of circRTN4 in bovine adipocytes, with a particular focus on primary subcutaneous preadipocytes derived from a fetal Qinchuan calf. We examined the effects of circRTN4 on preadipocyte proliferation, apoptosis, and adipogenic differentiation and further explored the potential involvement

of the miR-205/Lin9 regulatory pathway. This study aims to provide new insights into circRNA-mediated post-transcriptional regulation of bovine adipocyte development and to improve our understanding of the molecular mechanisms underlying bovine fat deposition.

In summary, this study aims to elucidate the function and molecular mechanism of circRTN4 in bovine adipocyte development, with a particular focus on primary subcutaneous preadipocytes, thereby providing further insight into the molecular regulation of bovine preadipocyte biology. The findings not only enrich our understanding of the regulatory role of circRNAs in bovine adipose tissue development but may also provide a reference for further investigations into the molecular mechanisms underlying adipogenesis in livestock species.

2. Materials and Methods

2.1. Samples

Tissue samples including muscle, adipose, liver, spleen, renal, galacyophore, skin and heart were collected from three individual cattle. Immediately after collection, each sample was placed into liquid nitrogen before being transferred to a −80 °C freezer.

Primary bovine preadipocytes were isolated from subcutaneous adipose tissue of a single fetal Qinchuan cattle. Fetal bovine subcutaneous adipose tissue was collected under sterile conditions after the external surface of the fetus had been disinfected with 75% ethanol, and then subcutaneous fat was harvested under sterile conditions for later use. Tissue pieces were rinsed twice with 75% ethanol and twice with PBS containing 2% penicillin-streptomycin, then minced in a dish with a small volume of complete medium (DMEM/F-12 with 20% FBS and 1% antibiotics). The minced tissue was digested in 0.2% collagenase I at 37 °C for 2 h with agitation. Following centrifugation, the pellet was washed with pre-warmed PBS and cultured in complete medium at 37 °C in 5% CO_2. Cells were passaged upon reaching about 80% confluence, and cells at passages 3–5 were used for all subsequent experiments.

When cell confluence reached approximately 100%, the medium was replaced with differentiation induction medium (complete medium supplemented with 10 μg/mL insulin, 1 μM dexamethasone, 0.5 mM IBMX, and 1 μM rosiglitazone) for induction. After 2 days of induction, the medium was removed and replaced with maintenance medium (complete medium containing 10 μg/mL insulin and 1 μM rosiglitazone), which was renewed every 2 days, cells were maintained under adipogenic induction/maintenance conditions for 9 days.

2.2. RNase R Tolerance Assay

To assess the RNase R resistance and support the circular nature of circRTN4, an RNase R digestion assay was performed. Total RNA extracted from bovine preadipocytes was incubated with or without 2 U/μg of RNase R in a total volume of 20 μL, supplemented with 2 μL of 10× RNase R Reaction Buffer. The reaction mixture was subsequently incubated at 37 °C for 15 min to facilitate the digestion of linear transcripts. For the control group, total RNA was treated under identical incubation conditions but with the omission of the RNase R enzyme. Following digestion, the remaining RNA from both the RNase R-treated and Mock groups was immediately subjected to cDNA synthesis using a reverse transcription kit. The relative abundance of circRTN4 and its linear counterpart RTN4 mRNA was quantified via real-time quantitative PCR (RT-qPCR). The linear β-actin transcript was employed as an internal control to monitor the digestion efficiency of linear RNAs.

2.3. Vector Construction and Transfection

The circRTN4 overexpression vector was constructed by cloning the full-length circRTN4 cDNA into the pCD25-ciR vector (GENESEED, Guangzhou, China, GS0106) (Figure S1). The Lin9 overexpression vector was constructed by cloning the full-length Lin9 cDNA into the pcDNA3.1 vector. miR-205 mimics and miR-205 inhibitor were obtained from GenePharma (Shanghai, China) (Table S1); siRNA and its negative control were also purchased from the same company (Table S2). Bovine preadipocytes were seeded in 6-well plates (for RNA/protein extraction) or 96-well plates (for CCK-8 and EdU assays) at densities of 2×10^5 cells/well and 5×10^3 cells/well, respectively, and cultured until reaching 70–80% confluence prior to transfection. All transfections were performed using Lipofectamine 2000 (Invitrogen, CA, USA) following the manufacturer's instructions. Briefly, for each well of a 6-well plate, 2.5 μg of plasmid DNA or 100 pmol of miRNA mimics/inhibitor or siRNA and 5 μL of Lipofectamine 2000 were separately diluted in 100 μL of Opti-MEM (Gibco, NY, USA), incubated at room temperature for 5 min, then mixed gently and incubated for an additional 15 min to allow complex formation. The complexes were added to the cells in fresh complete medium without antibiotics. After 6 h of incubation at 37 °C, the transfection medium was replaced with complete growth medium. For differentiation experiments, transfections were performed 24 h prior to adipogenic induction. No additional transfection was performed during the subsequent differentiation period. Following the initial transfection, cells were maintained under adipogenic induction conditions until day 9, when Oil Red O staining was performed to evaluate lipid accumulation. At 48 h post-transfection, cells were harvested for RT-qPCR and Western blot analysis. CCK-8 and EdU assays were carried out at 48 h post-transfection, while Oil Red O staining was conducted on days 9 of differentiation, respectively.

2.4. Real-Time Quantitative Polymerase Chain Reaction (RT-qPCR)

Total RNA was extracted using the Trizol (Accurate Biology, Shanghai, China, AG21101) method. Then, 1 μg of RNA was converted into cDNA using PrimeScript RT Enzyme (Accurate Biology, AG11705). SYBR qPCR Master Mix (Vazyme, Nanjing, China) was employed for RNA amplification and quantification. All primers were validated by melt curve analysis, and their sequences are listed in Table 1. β-actin was used as the reference gene for mRNA and circRNA expression analysis, whereas U6 was used as the internal reference for miRNA expression analysis. The ΔΔCT method was applied to determine target gene expression alterations, which were expressed as fold changes ($FC = 2^{-\Delta\Delta CT}$). Statistical analyses were performed using ΔCT values, whereas relative expression was presented as $2^{-\Delta\Delta CT}$.

Table 1. Primer sequence information.

Genes	Primer Sequences (5′ → 3′)	Product Size/bp
circRTN4	F: CAGCAATTCTGCTCTTGGTCA	202
	R: TGTAGGCCGTTACACTCACA	
RTN4	F: TTCCTTATGGCAGCACAGGAG	71
	R: TCCTCGGTCACCTTTGACAC	
β-actin	F: CATCCTGACCCTCAAGTA	91
	R: CTCGTTGTAGAAGGTGTG	
CDK2	F: CCCTGGATGAAGATGGACGG	126
	R: GGTGAGGTACTGGCTTGGTC	

Table 1. *Cont.*

Genes	Primer Sequences (5′ → 3′)	Product Size/bp
CDK4	F: GTGACAAGTGGTGGGACAGT	168
	R: GATACAGCCAACGCTCCACA	
CCND1	F: CCGTCCATGCGGAAGATC	108
	R: CAGGAAGCGGTCCAGGTAG	
CCNE1	F: GTGGCATTTAAGTCCCCTGA	100
	R: AGGATACTGAGGCAGGAGCA	
PCNA	F: TCCAGAACAAGAGTATAGC	94
	R: TACAACAGCATCTCCAAT	
PPARγ	F: AGGATGGGGTCCTCATATCC	121
	R: GCGTTGAACTTCACAGCAAA	
C/EBPα	F: TGGACAAGAACAGCAACGAG	130
	R: TTGTCACTGGTCAGCTCCAG	
C/EBPβ	F: TTCCTCTCCGACCTCTTCTC	79
	R: CCAGACTCACGTAGCCGTACT	
FABP4	F: GTGTCACTGCCACCAGAGTT	76
	R: GGAGTTCGATGCAAACGTCA	
Bcl2	F: ATGTGTGTGGAGAGCGTCAA	143
	R: GGGCCATACAGCTCCACAAA	
Bax	F: GAGATGAATTGGACAGTAACA	118
	R: TTGAAGTTGCCGTCAGAA	
BAD	F: GTCTCCTTCAAGGGGCTTCC	121
	R: AGCCTCCTCTCCCCAAGTTC	
caspase9	F: TGGTGGTCATCCTGTCTC	76
	R: CATCCATCTGTGCCATAAAC	
SMAD1	F: GGCACATCGGGAAAGGAGTT	134
	R: GCAAACGGTAGTGGGATGGA	
APOA2	F: CCAAGGGCTCAGAGCTTCAA	175
	R: TGAAGAAGGGCGTCAGTTCC	
XYLT1	F: TACCCCTCACGTTGTCGTTG	160
	R: GTTAGGAACGGAGGTGGCAA	
DST	F: AACTCCCTGTAAACCAGCCG	143
	R: TGGTGATCAAGCCACTGTCC	
HDX	F: TTGATGATCGGACACGCTGA	149
	R: TTGCCAACCCACGTCTCG	
Lin9	F: CAGGACAGCCCTGTGTTGAA	98
	R:GTCGCCTCCTTCTGCTAGAC	
miR-2291-RT	GTCGTATCCAGTGCAGGGTCCGAGGTATTCGCACTGGATAC-GACCTGCCC	

Table 1. *Cont.*

Genes	Primer Sequences (5′ → 3′)	Product Size/bp
miR-2291-F	CGGCTGATAGTGAGCGACTG	
miR-12039-RT	GTCGTATCCAGTGCAGGGTCCGAGGTATTCGCACTGGATACGACAGAGAA	
miR-12039-F	CCAGGGCCCTGGCTTC	
miR-205-RT	GTCGTATCCAGTGCAGGGTCCGAGGTATTCGCACTGGATACGACCAGACT	
miR-205-F	CGTCCTTCATTCCACCGG	
miR-2397-3p-RT	GTCGTATCCAGTGCAGGGTCCGAGGTATTCGCACTGGATACGACATGCGT	
miR-2397-3p-F	CGCAGAGCAGTGGCAAGA	
Universal miRNA reverse primer	AGTGCAGGGTCCGAGGTATT	
U6	F: CGAAACCACCACCACACT	
	R: GGATATGGACTGACTCAGGA	

2.5. Cell Proliferation and Apoptosis

Following transfection, primary bovine preadipocytes were cultured for 48 h before the CCK-8 assay. Three independent replicates were performed for each treatment group, with replicate wells included within each biological replicate. A total of 10 μL of CCK-8 reagent (Solarbio, Beijing, China) was added to each well and incubated for 2 h at 37 °C. An enzyme marker (BioTek, Winooski, VT, USA) measured the absorbance at 450 nm. Preadiocyte mitotic activity was monitored via the tracking of active DNA synthesis using an 5-ethynyl-2′-deoxyuridine (EdU) labeling toolkit (RiboBio, Guangzhou, China). Briefly, replicating cells were exposed to the EdU substrate, allowing the nucleotide analog to incorporate into the newly synthesized genomic DNA strands. The subsequent azide-alkyne cycloaddition was executed to conjugate the fluorophore, and the resulting fluorescently labeled nuclei were captured and visualized utilizing an inverted fluorescence microscope.

Apoptosis-related changes in bovine preadipocytes were assessed using a TUNEL apoptosis detection kit (Servicebio, Wuhan, China) according to the manufacturer's instructions. Briefly, cells were fixed with 4% paraformaldehyde for 20 min at room temperature and permeabilized with 0.1% Triton X-100 for 10 min. After washing with PBS, cells were incubated with the TUNEL reaction mixture for 1 h at 37 °C in the dark. Nuclei were counterstained with DAPI. Fluorescence images were captured under identical conditions, and the percentage of TUNEL-positive cells was calculated as the ratio of TUNEL-positive cells to total DAPI-positive cells. Three replicates were analyzed for each group.

2.6. Western Blotting Analysis

For Western blot analysis, total protein was extracted from bovine primary preadipocytes using RIPA lysis buffer supplemented with protease and phosphatase inhibitors. The lysates were incubated on ice for 30 min and centrifuged at 12,000× *g* for 15 min at 4 °C. The supernatants were collected, and equal amounts of protein were mixed with 5× loading buffer and denatured at 95 °C for 10 min. Equal amounts of proteins were separated in 12% sodium dodecyl sulfate-polyacrylamide gel electrophoresis at 110 V for 2 h, followed by transfer to polyvinylidene difluoride membranes at 250 mA current for 2.5 h. Membranes were blocked with 5% skim milk before incubation with the following antibodies: PCNA (1:2000; HUABIO, Hangzhou, China), CCND1 (1:500; HUABIO), Bax (1:2000; Abways

Technology, Shanghai, China), Caspase9 (1:1000; WANLEIBIO, Shenyang, China), Flag (1:10,000; Epizyme, Shanghai, China), and β-actin (1:2000; Proteintech, Wuhan, China), overnight at 4 °C. Afterward, reaction with secondary antibodies for 2 h at room temperature. Then, signal visualization was realized by a chemiluminescent system.

2.7. Oil Red O Staining

Intracellular lipid loading was visualized at the 9-day post-differentiation milestone using a lipophilic Oil Red O (#O0625, Sigma, St. Louis, MO, USA). The specific incorporation of the dye into the hydrophobic core of cellular vacuoles generated a robust histochemical readout. The stained cultures were then processed immediately for subsequent microscopic imaging and extraction. For quantification of fat droplet staining, the lipid droplets were dissolved in 100% isopropanol, and absorbance was read at 510 nm.

2.8. Dual-Luciferase Reporter Assay

The wild type (circRTN4-WT) and mutant type (circRTN4-MUT) without miR-205 binding site were cloned into the psiCHECK-2 vector, which confirmed that the cloning was successful. The wild type (Lin9-WT) and mutant type (Lin9-MUT) without miR-205 binding site were cloned into the psiCHECK-2 vector, which confirmed that the cloning was successful. These plasmids were transfected into miR-205 overexpressing HEK293T cells, and dual luciferase activity was measured by lysing HEK293T cells 24 h after transfection, according to the protocol. Renilla fluorescence and firefly fluorescence activity were measured using a microplate reader (SuPerMax 3100, Shanghai, China) [16].

2.9. Prediction of ORF and IRES in circRTN4

The potential coding capacity of circRTN4 was evaluated using bioinformatic analysis. The full-length sequence of circRTN4 was analyzed using circPrimer 2.0 to identify candidate ORFs. The predicted ORF sequence was translated into its corresponding amino acid sequence, and the theoretical molecular weight of the predicted peptide was calculated using the ExPASy ProtParam (https://web.expasy.org/protparam/) tool. Putative IRESs within circRTN4 were predicted using the IRES Detector. The identified ORF and IRES elements were used to assess the potential coding capacity of circRTN4 and to guide subsequent experimental validation.

2.10. Statistical Analyses

All cellular and molecular data are presented as mean ± standard deviation (SD) from three independent experimental replicates using cells derived from the same fetal donor. Mathematical modeling of the experimental boundaries was orchestrated via the SPSS 22.0 computational platform (SPSS, Chicago, IL, USA). A probability of 0.05 or less was considered statistically significant. * indicates $p < 0.05$, ** indicates $p < 0.01$.

3. Results

3.1. Characteristics of circRTN4 in Adipose Tissue

To validate the biogenesis of circRTN4, we verified its back-spliced junction, spanning exon 4 and exon 5 (347nt) of the RTN4 host gene, via PCR amplification and Sanger sequencing (Figure 1A). Moreover, circRTN4 showed greater resistance to RNase R digestion and maintained a relatively higher abundance than its linear counterpart following RNase R treatment (Figure 1B). These results support the RNase R resistance of circRTN4 and are consistent with its circular RNA characteristics. circRTN4 expression was detected in all examined bovine tissues, with a numerically higher level observed in adipose tissue; however, no significant tissue-specific difference was observed (Figure 1C). We next examined

circRTN4 expression during adipogenic differentiation. Its expression increased during differentiation, with the highest level observed at day 9 (Figure 1D). Taken together, these results confirm the circular characteristics of circRTN4 and demonstrate that its expression increases during bovine preadipocyte differentiation.

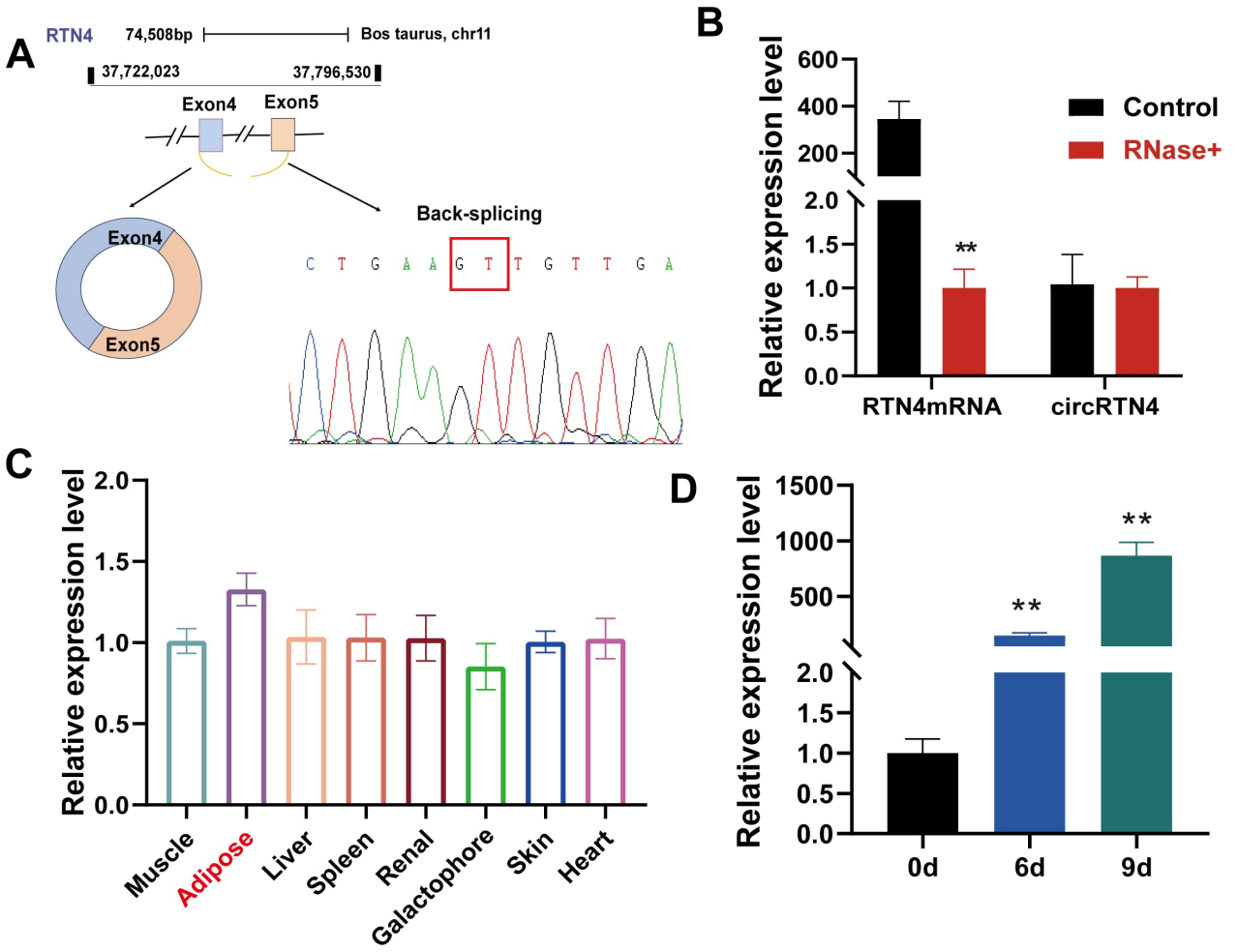


Figure 1. Characterizations of circRTN4. (**A**) Schematic of the structure of circRTN4. (**B**) Detection of circRTN4 and RTN4 mRNA expression in bovine precursor adipocytes after RNase R treatment. (**C**) Expression profile of circRTN4 in different bovine tissues. (**D**) Expression pattern of circRTN4 during different stages of bovine preadipocyte differentiation. Data are presented as mean ± SD. ** indicates $p < 0.01$.

3.2. circRTN4 Inhibits Preadipocyte Proliferation and Differentiation While Promoting Apoptosis

To examine the effects of circRTN4 on the biological functions of preadipocytes, the overexpression vector and siRNA of circRTN4 were successfully transfected into bovine primary preadipocytes. Critically, manipulating circRTN4 levels did not significantly alter the expression of its host gene RTN4 at the mRNA level, suggesting that the observed phenotypic changes are likely associated with circRTN4 itself rather than changes in its parental transcript (Figure 2A,B). Quantifying proliferation markers via RT-qPCR revealed that circRTN4 overexpression markedly suppressed PCNA, CDK2, CDK4, and CCND1 transcripts (Figure 2C), whereas its silencing consistently elevated their expression (Figure 2D). Furthermore, CCK-8 and EdU assays were used to further validate the inhibitory effect of circRTN4 on adipocyte proliferation. CCK-8 results showed that circRTN4 overexpression inhibited bovine preadipocyte viability, whereas circRTN4 interference promoted bovine

preadipocyte viability (Figure 2G). EdU results further demonstrated the inhibitory effect of circRTN4 on bovine adipocyte proliferation (Figure 2H,I).

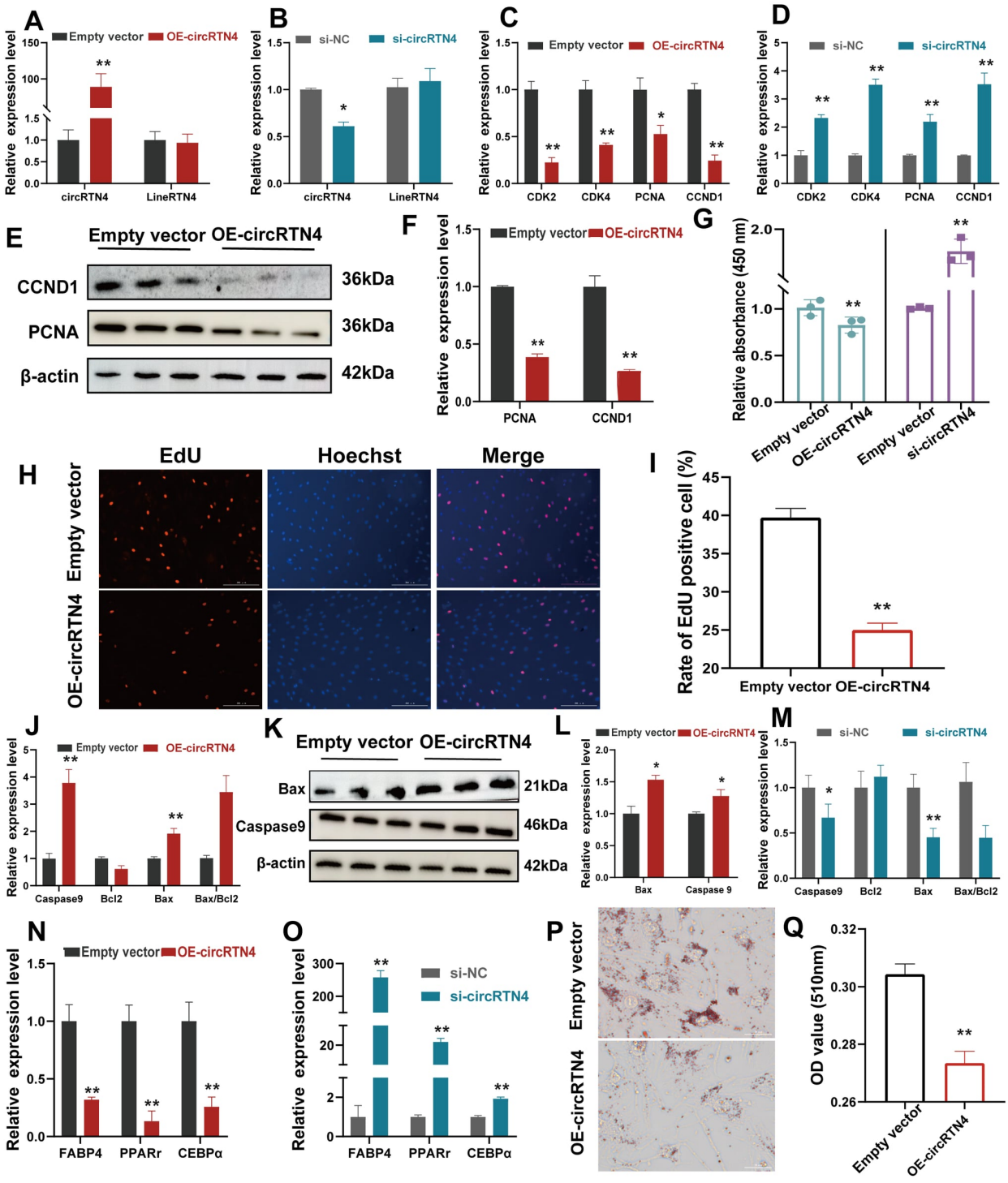


Figure 2. Effects of circRTN4 on proliferation, apoptosis, and adipogenic differentiation of bovine primary preadipocytes. (**A**,**B**) RT-qPCR analysis of host gene RTN4 expression following circRTN4 overexpression or knockdown. (**C**–**I**) Effects of circRTN4 on preadipocyte proliferation assessed. (**C**,**D**) RT-qPCR analysis. (**E**,**F**) WB analysis. (**G**) CCK-8 assay. (**H**,**I**) EdU incorporation. (**J**–**M**) Effects of circRTN4 on apoptosis assessed by apoptosis-related gene expression. (**N**–**Q**) Effects of circRTN4 on adipogenic differentiation assessed by adipogenic marker gene expression (**N**,**O**) and Oil Red O staining (**P**,**Q**). Data are presented as mean ± SD from three independent experiments. * $p < 0.05$, ** $p < 0.01$.

Prompted by these proliferation-related changes, we further investigated whether circRTN4 affects apoptosis-associated processes and adipogenic differentiation. The results showed that upon circRTN4 overexpression, the mRNA and protein levels of the apoptosis-related proteins Bax and caspase-9 were significantly upregulated (Figure 2J–L). Consistently, TUNEL staining showed a significant increase in the proportion of TUNEL-positive cells following circRTN4 overexpression (Figure S2A,B). Conversely, interference with circRTN4 downregulated the expression of the expression of caspase-9 (Figure 2M). Regarding terminal differentiation, RT-qPCR monitoring showed that circRTN4 overexpression blunted the expression of key adipogenic marker genes, whereas its knockdown elicited the inverse effect (Figure 2N,O). Oil Red O staining was also performed on day 9 to evaluate intracellular lipid accumulation. The results showed a modest reduction in lipid accumulation following circRTN4 overexpression (Figure 2P,Q). Although the changes in adipogenic marker gene expression were evident, the corresponding reduction in lipid accumulation was relatively modest, indicating that changes in marker gene expression did not translate proportionally into lipid accumulation at this time point. These findings suggest that circRTN4 negatively regulates bovine preadipocyte proliferation and adipogenic differentiation and may be involved in apoptosis-related processes.

3.3. Identification of CircRTN4 Coding Capacity

Since circRNAs lack a cap structure, their translation should occur through sequences that can function as internal ribosome entry sites (IRESs). Notably, bioinformatics analysis using an IRES detector identified the presence of an IRES in CircRTN4, suggesting its potential to encode a protein. To predict the coding potential of circRTN4, the ORF and IRES elements of circRTN4 were predicted using circPrimer2.0, and the results revealed that circRTN4 contains an ORF and an IRES (Figure 3A). Prediction using the Expasy ProtParam tool showed that the theoretical molecular weight of the protein encoded by circRTN4 is 4.1 kDa, and it was named circRTN4-35aa. After adding the Flag tag, its theoretical molecular weight is 5.1 kDa (Figure 3B). To verify the authenticity of the short peptide encoded by circRTN4, a recombinant circRTN4-Flag vector incorporating a Flag tag was constructed (Figure 3C). After transfection of the plasmid into bovine preadipocytes, fluorescence imaging confirmed good transfection efficiency in the circRTN4-Flag and OE-circRTN4 transfection groups (Figure 3D). Western blot analysis showed that β-actin was stably expressed in both the circRTN4-Flag and OE-circRTN4 groups, but the expected target band of 5.1 kDa was not detected using the Flag antibody (Figure 3E). These results indicated that no detectable FLAG-tagged peptide corresponding to the predicted circRTN4-derived peptide was observed under the experimental conditions. Although these results suggest that circRTN4 does not generate a readily detectable peptide product in bovine preadipocytes, further studies using specialized small-peptide detection systems are required to fully evaluate its protein-coding potential.

3.4. circRTN4 and miR-205 Exhibit a Potential Regulatory Relationship

We next investigated whether it acts as a ceRNA to regulate target gene expression by sponging miRNAs. Bioinformatic prediction identified several candidate miRNAs that potentially interact with circRTN4 (Figure S3A). The expression levels of these candidate miRNAs were subsequently examined following circRTN4 overexpression. Among the candidates tested, miR-205 showed a significant decrease in expression upon circRTN4 overexpression in bovine preadipocytes (Figure 4A), suggesting a potential regulatory relationship between circRTN4 and miR-205. Sequence alignment revealed complementary docking sites between circRTN4 and miR-205 (Figure S3B), and a dual-luciferase reporter

assay subsequently provided evidence consistent with a direct interaction between the two non-coding RNAs (Figure 4B).

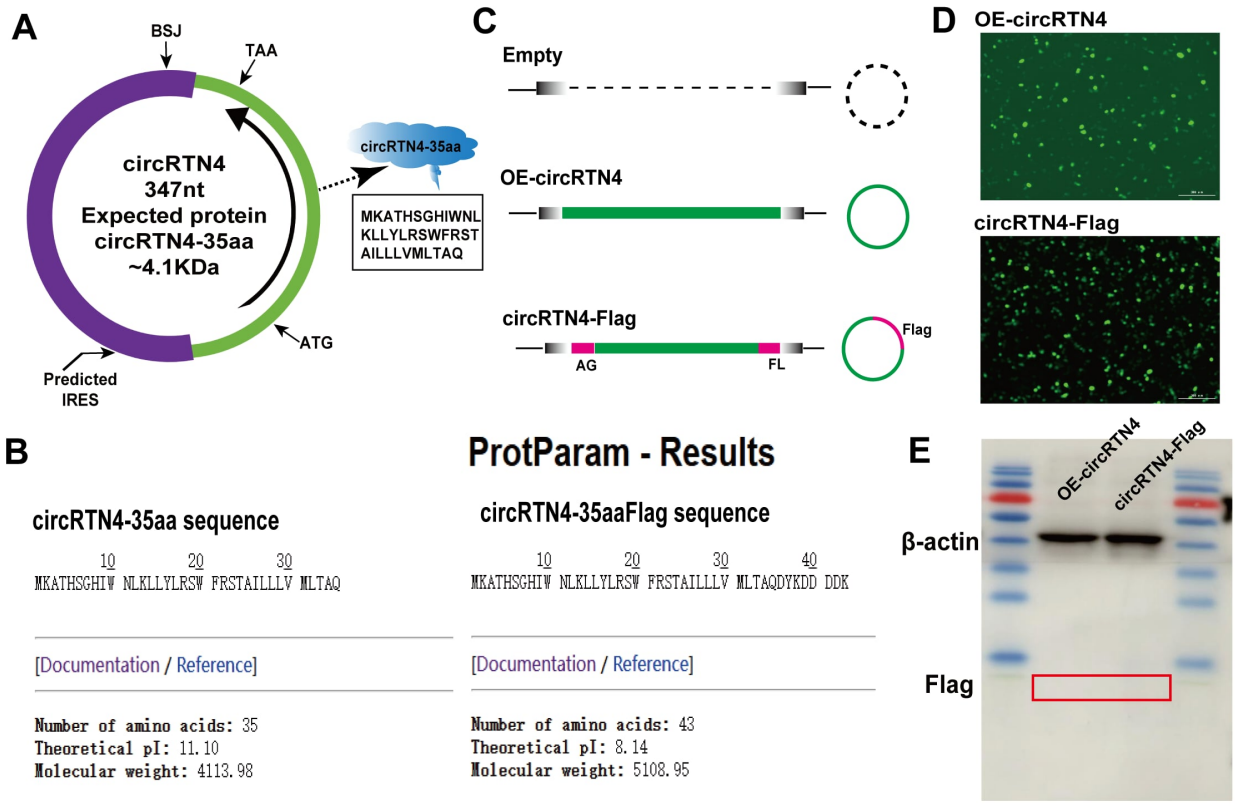


Figure 3. Prediction and experimental validation of the coding potential of circRTN4. (**A**,**B**) According to circPrimer 2.0 and Expasy circRTN4 is predicted to encode a specific polypeptide of 35aa. (**C**) Sketch showing the construction of the indicated vectors. (**D**) Fluorescence detection of transfection efficiency for circRTN4-Flag and OE-circRTN4. (**E**) Western blot analysis of circRTN4-Flag expression.

To decipher whether circRTN4 exerts its phenotype through this axis, we systematically characterized miR-205 function using over expression and inhibitor approaches (Figure 4C). Intriguingly, miR-205 overabundance drove an opposite phenotype to that of circRTN4. Enforced miR-205 expression upregulated mitotic marker genes (CDK2, CDK4, CCND1), enhanced PCNA and CCND1 protein accumulation, and boosted cell viability; conversely, miR-205 silencing suppressed these proliferative indices (Figure 4D–H). Furthermore, RT-qPCR and Western blot analyses revealed that miR-205 overexpression reduced the expression of apoptosis-related pro-apoptotic factors, whereas miR-205 knockdown showed the opposite effect (Figure 4I–L). Consistent with these molecular changes, TUNEL staining showed a decrease in the proportion of TUNEL-positive cells following miR-205 overexpression, whereas miR-205 knockdown resulted in an increase in TUNEL-positive cells (Figure S4A,B). Finally, RT-qPCR and Oil Red O staining demonstrated that miR-205 mimics advanced adipogenic differentiation and intracellular lipid accumulation, whereas its inhibition hindered adipogenesis (Figure 4M–P). Collectively, these results support a potential regulatory relationship between circRTN4 and miR-205 and indicate that miR-205 positively regulates bovine preadipocyte proliferation and adipogenic differentiation while being associated with reduced apoptotic cell death.

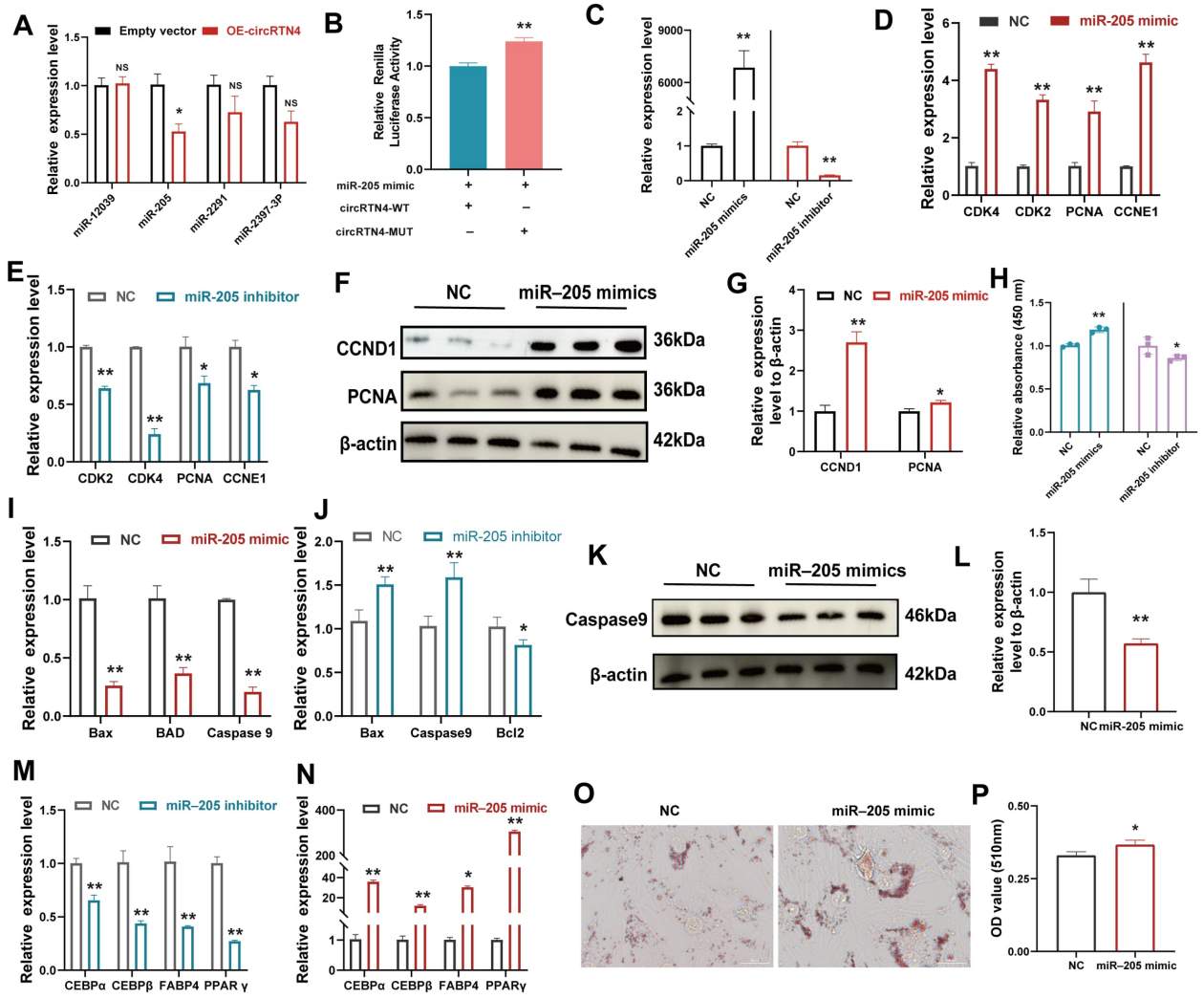


Figure 4. circRTN4–miR-205 interaction and functional effects of miR-205 in bovine primary preadipocytes. (**A**) RT-qPCR screening of candidate miRNAs following circRTN4 overexpression. (**B**) Dual-luciferase reporter assay validating the interaction between circRTN4 and miR-205. (**C**) Validation of miR-205 overexpression and knockdown efficiency. (**D**–**H**) Effects of miR-205 on preadipocyte proliferation assessed by proliferation-related gene and protein expression and CCK-8 assay. (**I**–**L**) Effects of miR-205 on apoptosis assessed by apoptosis-related gene and protein expression. (**M**–**P**) Effects of miR-205 on adipogenic differentiation assessed by adipogenic marker gene expression and Oil Red O staining. Data are presented as mean ± SD from three independent experiments. NS not significant, * $p < 0.05$, ** $p < 0.01$.

3.5. Lin9 Is a Candidate Downstream Target of miR-205

Potential target genes of miR-205 were predicted using the miRDB, miRWalk, and TargetScan databases, and 72 candidate genes were identified by intersection analysis (Figure 5A). Six candidate genes with high predicted binding scores were selected for experimental validation. miR-205 overexpression significantly decreased the expression of Lin9 and HDX, with Lin9 showing a clear response (Figure 5B). In addition, RT-qPCR analysis showed that Lin9 expression changed during bovine preadipocyte differentiation (Figure 5C), supporting its potential relevance to adipogenic differentiation. Lin9 was therefore selected for further investigation.

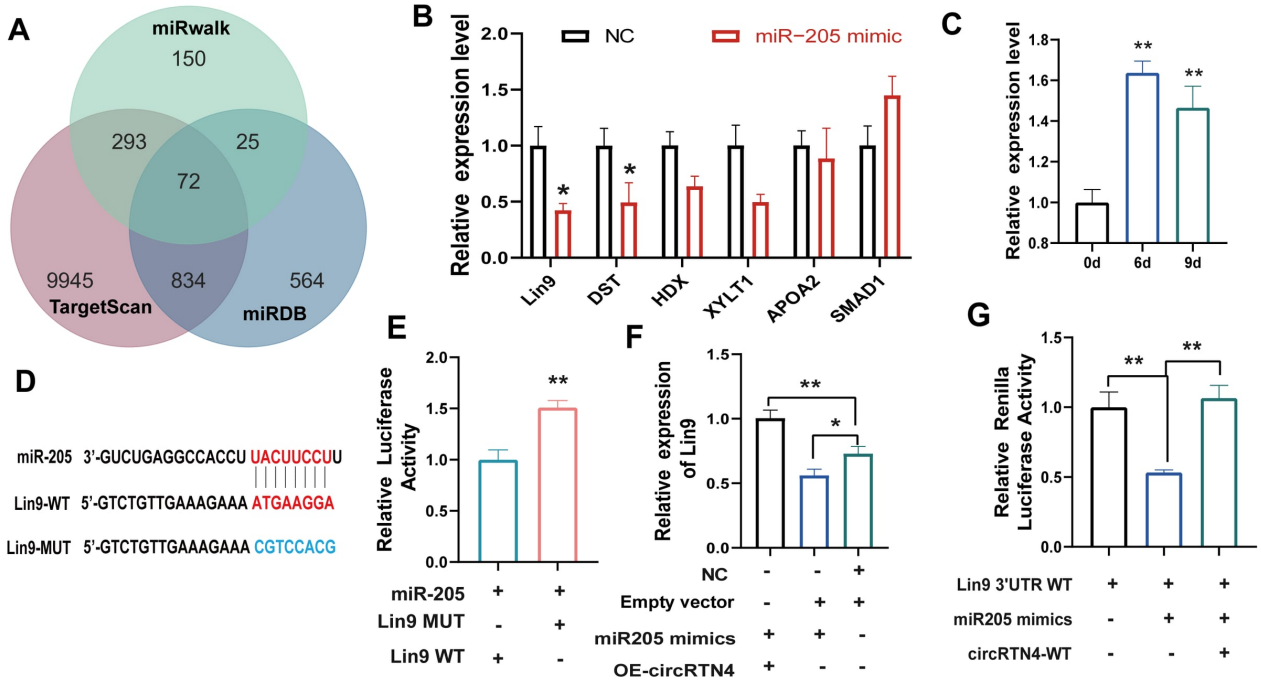


Figure 5. Lin9 is a candidate downstream target of miR-205. (**A**) Prediction of potential target genes of miR-205. (**B**) RT-qPCR analysis of candidate target gene. (**C**) Relative expression of Lin9 at different differentiation periods. (**D**) Construction of wild-type and mutant vectors of Lin9. (**E**) Results of dual-luciferase reporter assay. (**F**) Changes in Lin9 mRNA expression after co-transfection of OE-circRTN4 with miR-205. (**G**) Dual fluorescence assay to verify that circRTN4 competitively binds to miR-205 to regulate Lin9 expression. All data are presented as mean ± SD from three independent experiments. * indicates $p < 0.05$, ** indicates $p < 0.01$.

Sequence analysis identified a putative miR-205 binding site within the 3′UTR of Lin9 (Figure 5D). A dual-luciferase reporter assay showed that miR-205 significantly affected the activity of the Lin9 3′UTR-WT reporter, whereas mutation of the predicted binding site reduced this effect, supporting a sequence-dependent regulatory relationship between miR-205 and the Lin9 3′UTR (Figure 5E). We next examined whether circRTN4 was associated with miR-205-mediated regulation of Lin9. CircRTN4 overexpression partially alleviated the inhibitory effect of the miR-205 mimic on Lin9 mRNA expression (Figure 5F). Consistently, co-expression of circRTN4-WT reduced the inhibitory effect of the miR-205 mimic on the Lin9 3′UTR-WT reporter activity (Figure 5G). Collectively, these findings support a potential regulatory relationship among circRTN4, miR-205, and Lin9.

3.6. Lin9 Inhibits Preadipocyte Proliferation and Differentiation

We subsequently investigated the functional role of Lin9 in bovine preadipocytes (Figure 6A). Lin9 overexpression significantly reduced the expression of proliferation marker genes (Figure 6B–D), which was further supported by a significant decrease in cell viability detected by the CCK-8 assay (Figure 6E). In addition, Lin9 overexpression significantly increased the expression of the pro-apoptotic genes Bax and Caspase9 while decreasing Bcl2 expression (Figure 6F), accompanied by elevated BAX and Caspase9 protein levels (Figure 6G,H). Consistent with these changes, TUNEL staining showed a significant increase in the proportion of TUNEL-positive cells following Lin9 overexpression (Figure S5A,B). Furthermore, Lin9 overexpression significantly suppressed the expression of adipogenic differentiation marker genes (Figure 6I) and reduced lipid droplet accumulation in bovine preadipocytes, as demonstrated by Oil Red O staining (Figure 6J,K). These

findings identify Lin9 as a candidate downstream effector associated with the miR-205 regulatory pathway in bovine preadipocytes.

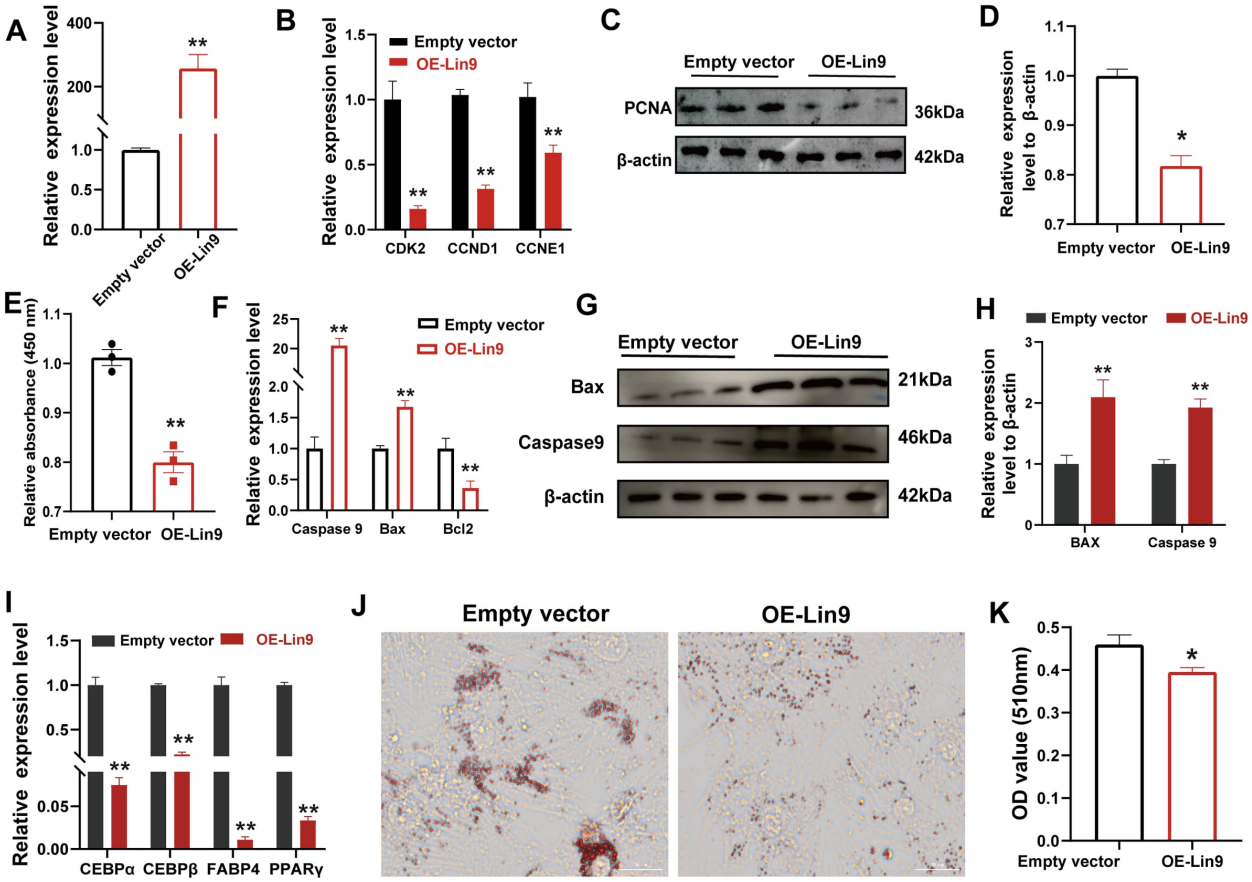


Figure 6. Lin9 suppresses bovine preadipocyte proliferation and differentiation and alters apoptosis-related responses. (**A**) Detection of Lin9 overexpression efficiency. (**B**) Detection of the expression of proliferation-related marker genes by qPCR after overexpression of Lin9. (**C**,**D**) Western blot analysis of Lin9 overexpression on proliferation marker genes (**C**) and quantification (**D**). (**E**) CCK-8 assay demonstrating that Lin9 overexpression significantly reduces bovine preadipocyte viability. (**F**) RT-qPCR analysis of apoptosis-related genes. (**G**,**H**) Western blot analysis (**G**) and quantification (**H**) of BAX and Caspase9 protein levels. (**I**) RT-qPCR analysis of differentiation marker genes after Lin9 overexpression. (**J**,**K**) Oil Red O staining (**J**) and quantification (**K**) of lipid droplets in differentiated preadipocytes. All data are presented as mean ± SD from three independent experiments. * indicates $p < 0.05$, ** indicates $p < 0.01$.

4. Discussion

CircRNAs are circular molecules produced by backward splicing of pre-mRNAs. Because they are covalently linked at the head and tail, circRNAs are difficult for RNA enzymes to destroy. With the advancement of sequencing in recent years, our understanding of circRNAs has also increased. Accumulating evidence indicates that circRNAs participate in various physiological processes. They can act as sponges to regulate the activity of miRNAs, encode functional short peptides, or bind to proteins to exert their functions [17]. Moreover, increasing evidence has demonstrated that circRNAs play important regulatory roles in adipose development and adipogenic differentiation [7,12,18]. However, the functional roles of individual circRNAs in bovine adipocyte biology remain incompletely understood. In this study, we identified a circRNA derived from the RTN4 gene in bovine preadipocytes, which we named circRTN4. We investigated the potential role of circRTN4

in bovine preadipocyte proliferation, differentiation, and apoptosis-related responses and explored its possible involvement in the circRTN4/miR-205/Lin9 regulatory axis. These findings provide further insight into circRNA-mediated post-transcriptional regulation during bovine preadipocyte development.

We confirmed that circRTN4 is generated by the back-splicing of exons 4 and 5 of the RTN4 gene using Sanger sequencing and RNase R digestion assays. CircRTN4 expression was detected in all examined bovine tissues, with no significant differences in expression among the examined tissues. Furthermore, the expression level of circRTN4 progressively increased during the differentiation of bovine preadipocytes, suggesting that circRTN4 may be associated with bovine preadipocyte differentiation. Notably, overexpression or knockdown of circRTN4 did not affect the mRNA expression level of its parental gene RTN4, suggesting that the observed phenotypic changes were not accompanied by detectable changes in the expression of the parental transcript. Functional assays suggested that circRTN4 negatively regulates bovine preadipocyte proliferation and differentiation and is associated with changes in apoptosis-related gene and protein expression. Similar regulatory functions on adipogenesis have also been reported in other circRNAs; in vitro experiments indicated that circSAMD4A affected differentiation by binding to miR-138-5p and regulating EZH2 expression [19]. In yak SRSF3 and hnRNP, A1-mediated m6A-modified circCDK14 regulates intramuscular fat deposition by acting as an miR-4492-z sponge [20]. Notably, the observed changes in apoptosis-related factors suggest that circRTN4 may contribute to the regulation of bovine preadipocyte biology, although the underlying effects on adipose tissue development require further investigation [21].

It is well established that circRNAs can exert their functions through various mechanisms, including serving as ceRNAs [22]. In addition to this mechanism, some circRNAs have also been reported to possess translation potential and generate functional short peptides under specific conditions [23]. However, this mechanism focuses on human disease research, for example, circSLC8a1 modulates the remodelling process of cardiac pressure overload by translating into a functional protein [24]. In cancer, the sequence of SPECC1-415aa, which is encoded by circSPECC1, can inhibit the binding of ANXA2 to EGFR by competitively binding to ANXA2 and inhibiting the phosphorylation of EGFR and AKT, thereby restoring the sensitivity of TMZ-resistant GBM cells to TMZ [25]. Based on this emerging mechanism, we predicted the potential IRES element and ORF within circRTN4 and identified a putative 35-amino-acid peptide. To investigate this possibility, we generated a Flag-tagged circRTN4 expression construct and performed Western blot analysis. Although no detectable FLAG-tagged peptide was observed at the predicted molecular weight, this result should be interpreted cautiously because conventional Western blot approaches have limitations in detecting very small peptides. Therefore, our current data do not provide evidence for detectable translation of circRTN4 under the conditions tested, while its potential coding capacity requires further validation using specialized approaches. The ceRNA hypothesis proposes that circRNAs can competitively bind to miRNAs through their miRNA response elements (MREs), thereby relieving the inhibitory effect of miRNAs on downstream target genes [26]. Currently, the ceRNA mechanism is widely recognized as the primary mode of action for many circRNAs, with typical examples including ciRS-7/CDR1as sponging miR-7 [27] and circHIPK3 sponging multiple miRNAs [28]. To investigate whether circRTN4 may act through a ceRNA-related mechanism, we first used bioinformatics prediction and dual-luciferase reporter assays to examine the potential interaction between circRTN4 and miR-205.

Our functional analyses suggested that miR-205 is associated with increased bovine preadipocyte proliferation and differentiation, accompanied by changes in apoptosis-related gene and protein expression. This pro-adipogenic effect is opposite to that reported in

certain cancer contexts, where miR-205 often functions as a tumor suppressor by targeting anti-apoptotic factors [29]. However, the tissue-specific functions of miRNAs have been widely documented; for example, miR-205 promotes proliferation of hair follicle stem cells but inhibits the growth of mammary epithelial cells [30,31]. In adipose tissue, a previous study reported that miR-205 promotes the proliferation and differentiation of 3T3 cells and identified GSK-3β as a target of miR-205 [32]. Because GSK-3β is a known regulator of Wnt signaling, these findings provide a possible context for the pro-adipogenic effects of miR-205. However, the GSK-3β/Wnt pathway was not directly examined in the present study. Therefore, the previous findings are considered supportive context rather than direct mechanistic evidence for the role of miR-205 in the bovine preadipocyte model used here. In the present study, our results instead support a regulatory relationship between miR-205 and Lin9.

To further characterize the downstream genes of the circRTN4/miR-205 regulatory axis, we used multiple databases for prediction and performed dual-luciferase reporter assays to support a sequence-dependent regulatory relationship between miR-205 and the Lin9 3′UTR. Lin9 is a core component of the DREAM complex (composed of DP, RB-like, E2F4, and MuvB), which represses the expression of cell cycle genes during quiescence and differentiation [33,34]. In this study, overexpression of Lin9 inhibited preadipocyte proliferation and differentiation while promoting apoptosis-associated changes. These findings are highly consistent with the established function of the DREAM complex in cell cycle exit and terminal differentiation [35]. Specifically, Lin9 is essential for proper cell cycle arrest during mouse embryogenesis and represses E2F target genes in senescent cells [33,36]. Given that adipogenic differentiation requires coordinated cell cycle exit and suppression of proliferation-associated gene expression, the transcriptional repression mediated by the DREAM complex may contribute to establishing a cellular state permissive for adipogenic differentiation [37]. Our findings suggest that miR-205-mediated repression of Lin9 may contribute to the increased proliferation and differentiation observed in bovine preadipocytes. Conversely, circRTN4 may interact with miR-205, potentially contributing to increased Lin9 expression and the inhibitory effects of circRTN4 on preadipocyte adipogenic activity. Therefore, the circRTN4/miR-205/Lin9 regulatory axis may provide a potential link between circRNA-mediated post-transcriptional regulation and Lin9-associated control of cell-cycle progression during bovine preadipocyte development.

Our findings support a potential regulatory relationship among circRTN4, miR-205, and Lin9. Several limitations of this study should be acknowledged. All cellular experiments were performed using bovine preadipocytes derived from a single fetal donor, which may limit the generalizability of the findings. Validation using cells from multiple independent donors is therefore needed. Then although our results suggest a potential circRTN4/miR-205/Lin9 regulatory relationship, rescue experiments and further validation of endogenous molecular interactions were not performed. Thus, the proposed ceRNA mechanism requires additional investigation. In particular, approaches such as AGO2-RIP and RNA pull-down assays could provide further evidence of the interactions among these molecules. Finally, the present study was conducted primarily in vitro, and the physiological relevance of this regulatory relationship in bovine adipose tissue remains to be investigated.

5. Conclusions

In summary, circRTN4 is a bovine circRNA derived from exons 4 and 5 of RTN4 and is associated with bovine preadipocyte differentiation. Functional analyses suggested that circRTN4 may negatively regulate preadipocyte proliferation and differentiation, with accompanying changes in apoptosis-related factors. Mechanistic analyses provided evidence for a potential regulatory relationship among circRTN4, miR-205, and Lin9, suggesting that

this pathway may contribute to the regulation of bovine preadipocyte biology (Figure 7). These findings provide additional insight into the potential role of circRNA-mediated post-transcriptional regulation in bovine adipogenesis.

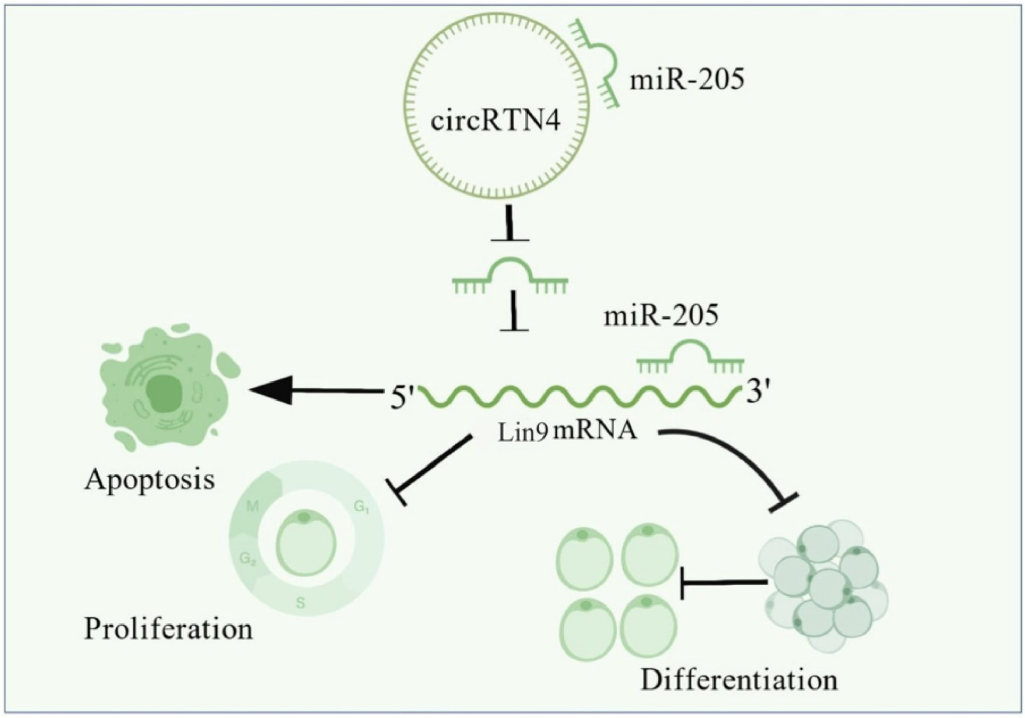


Figure 7. Schematic diagram of circRTN4 inhibition of bovine adipocyte proliferation and differentiation through miR-205/Lin9 axis.

Supplementary Materials: The following supporting information can be downloaded at: https://www.mdpi.com/article/10.3390/cells15222104/s1, Figure S1: pCD25-ciR plasmid profile; Figure S2: TUNEL staining following circRTN4 overexpression in bovine preadipocytes. (A) Representative images of TUNEL staining. (B) The proportion of TUNEL-positive cells was quantified; Figure S3: A circRTN4-miRNA interaction network map. B circRTN4 binding site prediction with miR-205; Figure S4: TUNEL staining following miR-205 overexpression in bovine preadipocytes. (A) Representative images of TUNEL staining. (B) The proportion of TUNEL-positive cells was quantified; Figure S5: TUNEL staining following Lin9 overexpression in bovine preadipocytes. (A) Representative images of TUNEL staining. (B) The proportion of TUNEL-positive cells was quantified; Table S1: miR-205 mimics and inhibitors and negative control sequences; Table S2: siRNA sequences.

Author Contributions: Y.L. (Yue Liu): Writing—review and editing, Writing—original draft, Investigation, Validation, Visualization. T.Y.: Writing—original draft, Investigation, Software, Formal analysis, Data curation. X.W.: Investigation, Visualization, Software. L.S.: Investigation, Validation. Z.H.: Software, Formal analysis. S.Z.: Formal analysis. C.P.: Conceptualization, Methodology. Y.L. (Yang Li): Conceptualization, Methodology. X.L.: Conceptualization, Funding acquisition, Methodology, Resources. E.J.: Writing—review and editing, Supervision, Conceptualization, Project administration. All authors have read and agreed to the published version of the manuscript.

Funding: We gratefully acknowledge the financial support provided by the following funding agencies: the Science Fund for Distinguished Young Scholars of Shaanxi Province (No. 2024JC-JCQN-30), the National Natural Science Foundation of China (No. 32372852; No. 32402717), and the Shaanxi Provincial Innovation Leadership Program in Sciences and Technologies for Young and Middle-aged Scientists (No. 2023SR205).

Institutional Review Board Statement: The study followed the guidelines of the "Management of Laboratory Animal Affairs" established by the Ministry of Science and Technology, with ethical

approval from the Ethics Committee of Northwest A&F University. Number: DK2022032; Time: 14 March 2022.

Informed Consent Statement: Not applicable.

Data Availability Statement: The data supporting the findings of this study are available from the corresponding authors upon reasonable request.

Acknowledgments: The authors gratefully acknowledge all collaborators who contributed to this work. AI-assisted tools (ChatGPT3.0, OpenAI) were used solely for language editing to improve clarity and conciseness. The tool was not used for study design, data analysis, or interpretation of results. All content was reviewed and approved by the authors.

Conflicts of Interest: The authors declare no conflicts of interest.

Abbreviations

The following abbreviations are used in this manuscript:

IMF	intramuscular fat
ncRNAs	non-coding RNAs
circRNAs	circular RNAs
RTN4	Reticulon 4
ceRNA	competing endogenous RNA
IRESs	Internal ribosome entry sites
ORF	open reading frame
MREs	miRNA response elements
Lin9	Lin-9 DREAM muvbcore Complex Component
RT-qPCR	real-time quantitative PCR
TMZ	temozolomide
GBM	Glioblastoma Multiforme

References

1. Tan, Z.; Pokhrel, B.; Zhou, Z.; Jiang, H. Transcriptome analysis unveils multiple reasons behind delayed and slower deposition of intramuscular fat compared to subcutaneous fat in cattle. *BMC Genom.* **2025**, *26*, 706. [CrossRef] [PubMed]
2. Frank, D.; Ball, A.; Hughes, J.; Krishnamurthy, R.; Piyasiri, U.; Stark, J.; Watkins, P.; Warner, R. Sensory and Flavor Chemistry Characteristics of Australian Beef: Influence of Intramuscular Fat, Feed, and Breed. *J. Agric. Food Chem.* **2016**, *64*, 4299–4311. [CrossRef] [PubMed]
3. Liu, S.; Yang, Y.; Luo, H.; Pang, W.; Martin, G.B. Fat deposition and partitioning for meat production in cattle and sheep. *Anim. Nutr.* **2024**, *17*, 376–386. [CrossRef] [PubMed]
4. Tang, Q.Q.; Lane, M.D. Adipogenesis: From stem cell to adipocyte. *Annu. Rev. Biochem.* **2012**, *81*, 715–736. [CrossRef] [PubMed]
5. Sakers, A.; De Siqueira, M.K.; Seale, P.; Villanueva, C.J. Adipose-tissue plasticity in health and disease. *Cell* **2022**, *185*, 419–446. [CrossRef] [PubMed]
6. Sleiman, L.; Dinescu, S. Role of Non-Coding RNAs in White and Brown Adipose Tissue Differentiation and Development. *Noncoding RNA* **2025**, *11*, 30. [CrossRef] [PubMed]
7. Jiang, E.; Zhang, C.; He, Z.; Zhang, Y.; Yang, Y.; Pan, C.; Jiang, F.; Song, E.; Zhang, S.; Lan, X. A novel A-to-G mutation in circBDP1 alters adipocyte proliferation and differentiation and affects bovine carcass traits. *J. Zhejiang Univ. Sci. B* **2026**, *27*, 918–922. [CrossRef] [PubMed]
8. Abebe, B.K.; Guo, J.; Wang, J.; Jilo, D.D.; Yu, S.; Cheng, G.; Li, A.; Zan, L. Exploring the regulatory mechanisms of differentially expressed circRNAs during bovine intramuscular adipogenic differentiation. *BMC Genom.* **2025**, *27*, 58. [CrossRef] [PubMed]
9. Wang, Y.; Cui, Y.; Li, X.; Jin, S.H.; Wang, H.; Gaipl, U.S.; Ma, H.; Wang, S.; Zhou, J.G. CircRNAs: Functions and emerging roles in cancer and immunotherapy. *BMC Med.* **2025**, *23*, 477. [CrossRef] [PubMed]
10. Rong, X.; Li, R.; Gong, T.; Li, H.; Zhao, X.; Cao, G.; Li, M.; Li, B.; Yang, Y.; Guo, X. CircMEF2C(2, 3) modulates proliferation and adipogenesis of porcine intramuscular preadipocytes by miR-383/671-3p/MEF2C axis. *iScience* **2024**, *27*, 109710. [CrossRef] [PubMed]
11. Tian, W.; Liu, Y.; Zhang, W.; Nie, R.; Ling, Y.; Zhang, B.; Zhang, H.; Wu, C. CircDOCK7 facilitates the proliferation and adipogenic differentiation of chicken abdominal preadipocytes through the gga-miR-301b-3p/ACSL1 axis. *J. Anim. Sci. Biotechnol.* **2023**, *14*, 91. [CrossRef] [PubMed]

12. Zhang, S.; Jiang, E.; Kang, Z.; Bi, Y.; Liu, H.; Xu, H.; Wang, Z.; Lei, C.; Chen, H.; Lan, X. CircRNA Profiling Reveals an Abundant circBDP1 that Regulates Bovine Fat Development by Sponging miR-181b/miR-204 Targeting Sirt1/TRARG1. *J. Agric. Food Chem.* **2022**, *70*, 14312–14328. [CrossRef] [PubMed]
13. Schwab, M.E. Functions of Nogo proteins and their receptors in the nervous system. *Nat. Rev. Neurosci.* **2010**, *11*, 799–811. [CrossRef] [PubMed]
14. Wong, C.H.; Lou, U.K.; Fung, F.K.; Tong, J.H.M.; Zhang, C.H.; To, K.F.; Chan, S.L.; Chen, Y. CircRTN4 promotes pancreatic cancer progression through a novel CircRNA-miRNA-lncRNA pathway and stabilizing epithelial-mesenchymal transition protein. *Mol. Cancer* **2022**, *21*, 10. [CrossRef] [PubMed]
15. Litovchick, L.; Sadasivam, S.; Florens, L.; Zhu, X.; Swanson, S.K.; Velmurugan, S.; Chen, R.; Washburn, M.P.; Liu, X.S.; DeCaprio, J.A. Evolutionarily conserved multisubunit RBL2/p130 and E2F4 protein complex represses human cell cycle-dependent genes in quiescence. *Mol. Cell* **2007**, *26*, 539–551. [CrossRef] [PubMed]
16. Wang, J.P.; Li, Q.Y.; Wang, Z.Y.; Zhang, S.; Bekana, K.; Zhang, Q.F.; Zheng, J.S.; Xu, Y.H.; Lan, X.Y.; Pan, C.Y. LncRSFD Alternative Splicing Modulates the Proliferation and Differentiation of Adipocytes Through Sponging miRNAs. *Anim. Res. One Health* **2026**, *4*, 407–418. [CrossRef]
17. Zhang, C.; Yu, Z.; Yang, S.; Liu, Y.; Song, J.; Mao, J.; Li, M.; Zhao, Y. ZNF460-mediated circRPPH1 promotes TNBC progression through ITGA5-induced FAK/PI3K/AKT activation in a ceRNA manner. *Mol. Cancer* **2024**, *23*, 33. [CrossRef] [PubMed]
18. Yang, Y.T.; Zhang, S.L.; Chen, L.; He, Y.; Jiang, E.H.; Pan, C.Y.; Li, Y.; Lei, C.Z.; Wu, J.Y.; Lan, X.Y. CircMED17 regulates bovine adipogenesis and fat deposition via mediating the proliferation and differentiation of bovine adipocytes. *J. Zhejiang Univ. Sci. B* **2026**, *27*, 1153–1170. [CrossRef] [PubMed]
19. Liu, Y.; Liu, H.; Li, Y.; Mao, R.; Yang, H.; Zhang, Y.; Zhang, Y.; Guo, P.; Zhan, D.; Zhang, T. Circular RNA SAMD4A controls adipogenesis in obesity through the miR-138-5p/EZH2 axis. *Theranostics* **2020**, *10*, 4705–4719. [CrossRef] [PubMed]
20. Qin, C.; Xu, F.; Yue, B.; Zhong, J.; Chai, Z.; Wang, H. SRSF3 and hnRNP A1-mediated m6A-modified circCDK14 regulates intramuscular fat deposition by acting as miR-4492-z sponge. *Cell. Mol. Biol. Lett.* **2025**, *30*, 26. [CrossRef] [PubMed]
21. Zhang, Y.; Huang, C. Targeting adipocyte apoptosis: A novel strategy for obesity therapy. *Biochem. Biophys. Res. Commun.* **2012**, *417*, 1–4. [CrossRef] [PubMed]
22. Firoozi, Z.; Shahi, A.; Mohammadisoleimani, E.; Afzali, S.; Mansoori, B.; Bahmanyar, M.; Mohaghegh, P.; Dastsooz, H.; Pezeshki, B.; Nikfar, G.; et al. CircRNA-associated ceRNA networks (circCeNETs) in chronic obstructive pulmonary disease (COPD). *Life Sci.* **2024**, *349*, 122715. [CrossRef] [PubMed]
23. Yi, Q.; Feng, J.; Lan, W.; Shi, H.; Sun, W.; Sun, W. CircRNA and lncRNA-encoded peptide in diseases, an update review. *Mol. Cancer* **2024**, *23*, 214. [CrossRef] [PubMed]
24. Li, F.; Du, W.W.; Li, X.; Wen, S.; Xu, J.; Yang, Q.; Zhang, C.; Ye, T.; Wei, J.; Wang, S. A new protein isoform encoded by human circular RNA circSLC8a1 contributes to cardiac remodelling. *Cardiovasc. Res.* **2025**, *121*, 882–899. [CrossRef] [PubMed]
25. Wei, C.; Peng, D.; Jing, B.; Wang, B.; Li, Z.; Yu, R.; Zhang, S.; Cai, J.; Zhang, Z.; Zhang, J.; et al. A novel protein SPECC1-415aa encoded by N6-methyladenosine modified circSPECC1 regulates the sensitivity of glioblastoma to TMZ. *Cell. Mol. Biol. Lett.* **2024**, *29*, 127. [CrossRef] [PubMed]
26. Salmena, L.; Poliseno, L.; Tay, Y.; Kats, L.; Pandolfi, P.P. A ceRNA hypothesis: The Rosetta Stone of a hidden RNA language? *Cell* **2011**, *146*, 353–358. [CrossRef] [PubMed]
27. Hansen, T.B.; Jensen, T.I.; Clausen, B.H.; Bramsen, J.B.; Finsen, B.; Damgaard, C.K.; Kjems, J. Natural RNA circles function as efficient microRNA sponges. *Nature* **2013**, *495*, 384–388. [CrossRef] [PubMed]
28. Zheng, Q.; Bao, C.; Guo, W.; Li, S.; Chen, J.; Chen, B.; Luo, Y.; Lyu, D.; Li, Y.; Shi, G.; et al. Circular RNA profiling reveals an abundant circHIPK3 that regulates cell growth by sponging multiple miRNAs. *Nat. Commun.* **2016**, *7*, 11215. [CrossRef] [PubMed]
29. Alla, V.; Kowtharapu, B.S.; Engelmann, D.; Emmrich, S.; Schmitz, U.; Steder, M.; Pützer, B.M. E2F1 confers anticancer drug resistance by targeting ABC transporter family members and Bcl-2 via the p73/DNp73-miR-205 circuitry. *Cell Cycle* **2012**, *11*, 3067–3078. [CrossRef] [PubMed]
30. Wang, D.; Zhang, Z.; O'Loughlin, E.; Wang, L.; Fan, X.; Lai, E.C.; Yi, R. MicroRNA-205 controls neonatal expansion of skin stem cells by modulating the PI(3)K pathway. *Nat. Cell Biol.* **2013**, *15*, 1153–1163. [CrossRef] [PubMed]
31. Chao, C.H.; Chang, C.C.; Wu, M.J.; Ko, H.W.; Wang, D.; Hung, M.C.; Yang, J.Y.; Chang, C.J. MicroRNA-205 signaling regulates mammary stem cell fate and tumorigenesis. *J. Clin. Investig.* **2014**, *124*, 3093–3106. [CrossRef] [PubMed]
32. Yu, J.; Chen, Y.; Qin, L.; Cheng, L.; Ren, G.; Cong, P.; Mo, D.; He, Z. Effect of miR-205 on 3T3-L1 preadipocyte differentiation through targeting to glycogen synthase kinase 3 beta. *Biotechnol. Lett.* **2014**, *36*, 1233–1243. [CrossRef] [PubMed]
33. Litovchick, L.; Florens, L.A.; Swanson, S.K.; Washburn, M.P.; DeCaprio, J.A. DYRK1A protein kinase promotes quiescence and senescence through DREAM complex assembly. *Genes Dev.* **2011**, *25*, 801–813. [CrossRef] [PubMed]
34. Esterlechner, J.; Reichert, N.; Iltzsche, F.; Krause, M.; Finkernagel, F.; Gaubatz, S. LIN9, a subunit of the DREAM complex, regulates mitotic gene expression and proliferation of embryonic stem cells. *PLoS ONE* **2013**, *8*, e62882. [CrossRef] [PubMed]

35. Ma, Y.; McKay, D.J.; Buttitta, L. Changes in chromatin accessibility ensure robust cell cycle exit in terminally differentiated cells. *PLoS Biol*. **2019**, *17*, e3000378. [CrossRef] [PubMed]
36. Reichert, N.; Wurster, S.; Ulrich, T.; Schmitt, K.; Hauser, S.; Probst, L.; Götz, R.; Ceteci, F.; Moll, R.; Rapp, U.; et al. Lin9, a subunit of the mammalian DREAM complex, is essential for embryonic development, for survival of adult mice, and for tumor suppression. *Mol. Cell Biol*. **2010**, *30*, 2896–2908. [CrossRef] [PubMed]
37. Sadasivam, S.; DeCaprio, J.A. The DREAM complex: Master coordinator of cell cycle-dependent gene expression. *Nat. Rev. Cancer* **2013**, *13*, 585–595. [CrossRef] [PubMed]

Disclaimer/Publisher's Note: The statements, opinions and data contained in all publications are solely those of the individual author(s) and contributor(s) and not of MDPI and/or the editor(s). MDPI and/or the editor(s) disclaim responsibility for any injury to people or property resulting from any ideas, methods, instructions or products referred to in the content.